Revista Chilena de Historia Natural
74:283-292, 2001

Effects of UV on photosynthesis of Antarctic phytoplankton: models and their application to coastal and pelagic assemblages

Efecto de la radiación UV sobre la fotosíntesis de fitoplancton antártico: modelos y su aplicación a ensambles costeros y pelágicos

PATRICK J. NEALE[1], JENNIFER J. FRITZ[1] & RICHARD F. DAVIS[2]

[1]Smithsonian Environmental Research Center, P.O. Box 28, Edgewater, Maryland 21037, U.S.A., e-mail: Neale@serc.si.edu
[2]Department of Oceanography, Dalhousie University, Halifax, Nova Scotia, B3H 4J1, Canada

ABSTRACT

We have characterized the photosynthetic response to ultraviolet radiation (UV) of natural phytoplankton assemblages in Antarctic (Southern Ocean) waters. Biological weighting functions (BWFs) and exposure response curves for inhibition of photosynthesis by UV were measured during spring-time ozone depletion (October-November). Two different models were developed to relate photosynthesis to UV exposure. A model that is a function of the duration of exposure (BWF_H) applied to assemblages in the well-mixed open waters of the Weddell-Scotia Confluence (WSC, 60° S, 50° W), since responses were a function of cumulative exposure and recovery rates were slow. These assemblages had a variable but generally high sensitivity to UV. A steady-state model (BWF_E) applied in the shallow waters near the Antarctic Peninsula (Palmer Station, 64° S, 64° W), where inhibition was a function of irradiance (reciprocity failed), and recovery was rapid. Using information on the time-dependence of photosynthesis in assemblages with active repair, inferences were drawn on the relative contribution of damage and recovery processes to the UV weights. BWFs for Palmer phytoplankton sampled during periods of pack-ice cover had both higher damage and higher repair than BWFs for WSC assemblages. BWFs for Palmer phytoplankton sampled during open water periods had about the same damage weights as Weddell-Scotia assemblages but had a higher repair rate. Solar exposures of more than 10 min were predicted to have generally less effect on Palmer phytoplankton than the WSC phytoplankton.

Key words: Southern Ocean, primary productivity, ozone depletion, photosynthesis-irradiance curves, biological weighting functions.

RESUMEN

Se caracterizó la respuesta fotosintética a radiación ultravioleta (RUV) en poblaciones naturales de fitoplancton del Océano Antártico. Se midieron las funciones espectrales de peso biológico (BWFs) y curvas de inhibición de fotosíntesis en respuesta a la exposición de RUV durante la temporada de mayor disminución de la capa de ozono (octubre-noviembre). Se desarrollaron dos modelos distintos que relacionan fotosíntesis con exposición a RUV. Un modelo considera la curva de respuesta al tiempo de exposición (BWF_H) debido a que se observo que las respuestas dependían de la exposición acumulativa y que la velocidad de recuperación fotosintéticas era lenta. Este modelo se aplica a poblaciones de fitoplancton residentes en mar abierto y en las aguas turbulentas de la Confluencia Weddell-Scotia (WSC, 60° S, 50° O). Estas poblaciones tienen una sensibilidad a la RUV variable y generalmente alta. El segundo modelo analiza el estado de equilibrio (BWF_E) y se aplica a las comunidades residentes en aguas poco profundas cerca de la Península Antártica (Estación Palmer, 64° S, 64° O), donde la inhibición dependió de la irradiación (reciprocidad falló), y donde la recuperación fue rápida. Usando la información derivada de la dependencia al tiempo de fotosíntesis en poblaciones con recuperación rápida, se pudo inferir la contribución relativa de procesos de daño y recuperación al peso espectral de la RUV. El método se aplicó a datos preliminares obtenidos en la Estación Palmer. Las BWFs de poblaciones recolectadas en Palmer cuando la capa de hielo que cubre las aguas es compacta asignaron más peso al daño y a una alta recuperación que las BWFs determinadas para poblaciones de WSC. Las BWFs de muestras de fitoplancton de Palmer durante el periodo de aguas abiertas tienen el mismo peso al daño que en aquellas de poblaciones de WSC aun cuando tienen una velocidad de recuperación más alta. Se predice que la exposición solar por más de 10 min en general tiene menos efecto sobre el fitoplancton de Palmer que sobre el fitoplancton de WSC.

Palabras clave: Océano Antártico, productividad primaria, disminución del ozono, curvas fotosíntesis-irradiación, funciones de peso biológico.

INTRODUCTION

Exposure to ultraviolet radiation (UV, 280-400 nm) is an inescapable "cost-of-business" for organisms inhabiting near-surface marine environments. The damaging potential of UV has been known since early research on marine photosynthesis (Steemann-Nielsen 1964), but full-scale investigation of the topic only got underway following the recent decline in stratospheric ozone and increases in exposure to UV, specifically the biologically damaging UV-B which is variously defined as 280-315 nm or 280-320 nm. A special focus has been given to the effects of UV on phytoplankton photosynthesis in the Southern Ocean, which is regularly exposed to the Antarctic "ozone hole" (Weiler & Penhale 1994). In situ incubations using broad-band filters that exclude either just UV-B or UV-B and UV-A (320-400 nm) have shown that photoinhibition of photosynthesis in the Antarctic and other environments is mostly due to naturally occurring UV, with the effects of UV-A dominating (Maske 1984, Bühlmann et al. 1987, Helbling et al. 1992, Prézelin et al. 1994, Villafañe et al. 1995, Furgal & Smith 1997).

The importance of UV exposure to aquatic photosynthesis has motivated development of models that define how inhibition may increase with ozone depletion or be affected by changes in the UV transparency of natural waters (largely a function of dissolved organic carbon) (Cullen & Neale 1997, Neale 2000). These environmental changes bring about wavelength-dependent changes in UV, and in order to understand the biological effects of those changes, wavelength-dependent weighting functions are required (Caldwell et al. 1986, Coohill 1989). Spectral weighting functions provide an approach to properly scale different exposure spectra for their 'effectiveness' at inhibiting photosynthesis. The concept is analogous to computing a weighted average of a UV spectrum, in that the weighting coefficients emphasize the shorter (more damaging) wavelengths relative to the long wavelengths. The approach is to calculate a single measure of inhibitory irradiance, E*, by summing the product of spectral exposure, $\varepsilon(\lambda)$, and a scaling coefficient or weight, $\varepsilon(\lambda)$, over a series of narrow wavelength bands ($\Delta\lambda$):

$$E^* = \sum_{\lambda=280\,nm}^{400\,nm} \varepsilon(\lambda) \cdot E(\lambda) \cdot \Delta\lambda \quad (1)$$

If the $\varepsilon(\lambda)$ are chosen correctly, then inhibition will be the same function of E* independent of the spectral composition.

Since definition of inhibition is sought over narrow bands ($\Delta\lambda$), exposure to narrow bandwidth (monochromatic) radiation may seem like the most accurate way to define a response spectrum. However, responses to UV reflect an interplay between damage and repair processes in living organisms (Vincent & Neale 2000). Here we use "repair" in a generic sense as all those processes that restore or reactivate photosynthetic function. The activity of several mechanisms influencing repair in phytoplankton, such as photosynthesis and photoenzymatic repair, are dependent upon concurrent exposure to UV-A and PAR. Thus, monochromatic exposures may not result in environmentally relevant weighting functions. To be more representative of biological responses to environmental UV, measurements are made using treatments composed of a range of wavelengths (i.e. with polychromatic sources). The basic approach is to generate a set of spectra using cutoff filters, i.e., filters which pass longer wavelength light starting at successively shorter cutoff wavelengths (Caldwell et al. 1986). The tradeoff for greater realism is that effects can no longer be precisely attributed to specific wavelengths. Instead, the weights are composites of the effects at that wavelength and the interactive effects of other wavelengths (Coohill 1991).

The presence or absence of repair also affects the time course of UV effects during exposure and thus how weighted exposure (equation 1) is translated into overall effect, e.g., a decrease in photosynthetic rate (P). A function describing the variation of effect with exposure is called an "Exposure Response Curve" (ERC). In the absence of repair, the time course of effects will be described by an exponential "survival curve" (Harm 1980),

$$P(t) = P_0 e^{-H^*}$$
$$H^* = \int E^* \partial t \quad (2)$$

where P(t) is photosynthetic rate, initially at level P_0, after a period, t, during which the integrated weighted exposure is H*. This ERC was consistent with inhibition of photosynthesis in deeply mixed assemblages of Antarctic phytoplankton (Neale et al. 1998b).

A contrasting behavior was found in cultures of a marine diatom growing at 20 °C that were exposed to different irradiances of supplementary UV-B for periods of 15 min to 4 h (Lesser et al. 1994). The rate of photosynthesis declined in response to UV-B, and within about 30 min reached a rate that was maintained for the remainder of the experiment. The time-course was consistent with a ERC in which repair (r) is proportional to the extent of inhibition (Lesser et al. 1994):

$$\frac{\partial P}{\partial t} = -kP + r(P_0 - P) \quad (3)$$

A steady-state $\partial P / \partial t = 0$ is eventually reached which is a function of the ratio of damage (k) and repair (r) rates (s^{-1}):

$$\frac{P}{P_0} = \frac{r}{(r+k)} = \frac{1}{(1+\frac{k}{r})} \quad (4)$$

The hyperbolic function specified by equation 4 described the steady-state rates of photosynthesis in the laboratory culture under UV+PAR exposure consistent with a dynamic balance between damage and repair (Lesser et al. 1994). The steady-state rate of photosynthesis depends on k which in turn depends on UV exposure rate (weighted irradiance).

The two exposure response models described above have been used to develop two types of BWFs for application to Antarctic phytoplankton. If repair is active and the exposures are sufficiently long to attain steady-state, the correct approach is to weight irradiance ($E(\lambda)$, mW m^{-2} nm^{-1}) and predict response as a hyperbolic function of weighted irradiance. This approach was taken to develop an integrated model of photosynthetic response to UV and PAR (i.e., the BWF-PI model), with weightings, $\varepsilon(\lambda)$, having units of reciprocal mW m^{-2} (Cullen et al. 1992). In this model, the achieved rate of photosynthesis (P^B, gC gChl h^{-1}) is the product of a potential rate in the absence of UV(P^B_{pot}) and the ERC for UV and PAR inhibition:

$$P^B = \frac{P^B_{pot}}{1 + E^*_{inh}}$$
$$E^*_{inh} = \sum_{\lambda=280\,nm}^{700\,nm} \varepsilon(\lambda) \cdot E(\lambda) \cdot \Delta\lambda \quad (5)$$

Since the spectral variation of $\varepsilon(\lambda)$ within PAR is not being investigated, a single average weighting coefficient is defined for the whole PAR spectrum (ε_{PAR}). This BWF-PI model was modified for the case when repair is not active (equation 2 applies) and the objective was to predict average photosynthetic rate over a specific exposure period (Neale et al. 1998b). In this case, we weight radiant exposure ($H(\lambda)$, J m^{-2} nm^{-1}) to compute weighted exposure for inhibition, H^*_{inh}, using a similar equation as for E^*_{inh}:

$$H^*_{inh} = \sum_{\lambda=280\,nm}^{700\,nm} \varepsilon_H(\lambda) \cdot H(\lambda) \cdot \Delta\lambda \quad (6)$$

where $H(\lambda) = \int E(\lambda) \cdot dt$. The weightings, ε_H (reciprocal J m^{-2}), define the effects of radiant exposure in contrast to irradiance. The average P^B over the period of cumulative exposure is obtained by integrating the ERC (equation 2):

$$P^B_{avg} = P^B_{pot} \cdot \frac{(1 - e^{-H^*_{inh}})}{H^*_{inh}} \quad (7)$$

This second model is termed the BWF_H -PI model because of the dependence on H, compared to the earlier BWF_E -PI model (with weights ε_E). Thus for the case of photosynthesis models, the type of BWF defined depends strongly on which ERC is applied. To accurately define both of these functions, observations will usually be needed of the variation in UV effects in relation to both varying spectral composition (for the BWF) and exposure times (for the ERC).

Measurements of photosynthesis during time courses and under 72 polychromatic UV-PAR treatments defined the BWF_E -PI model for cultures of diatoms and dinoflagellates at 20 °C (Cullen et al. 1992). More recently, time course and spectral response data have been measured for phytoplankton assemblages in a temperate estuary (Banaszak & Neale 2001) and as shown below, from the vicinity of Palmer Station. As in the previous culture measurements, photosynthesis by these assemblages attained a steady-state level during UV+PAR exposure, and thus photosynthesis was modeled using the BWF_E -PI approach. In sharp contrast, recovery processes made a negligible contribution to the response of phytoplankton sampled from the open waters of Weddell-Scotia Confluence (WSC) in the Southern Ocean (Neale et al. 1998b). Photosynthesis continuously declined during time-courses of UV exposure and rates remained low even after return to a benign irradiance regime. Consequently, the BWF_H-PI model was applied in which the cumulative effect of inhibition is described as the integral of a semi-logarithmic survival curve. Further discussion of these models and their application can be found in (Cullen & Neale 1997, Neale 2000).

Both of these models are useful descriptors of inhibition processes occurring in Antarctic and other phytoplankton assemblages. However, their application has resulted in the development of two classes of spectral weighting functions that cannot be directly compared. In this report we further develop the relationship between the two models and illustrate the application using previous results from the WSC and preliminary data from coastal phytoplankton assemblages sampled in the vicinity of Palmer Station.

MATERIAL AND METHODS

Measurements of photosynthesis

Water samples were taken in the vicinity of Palmer Station (64° S, 64° W) during October through December of 1997. These were taken by either a Niskin bottle during open water conditions, or using a clean bucket in the presence of pack ice. The ice was pushed aside in the latter case to exclude ice (and associated ice-algae) from the sample. Photosynthesis as a function of PAR and UV was determined from incorporation of ^{14}C-HCO_3 into acid-stable organic compounds during 1 h exposures in a specially designed spectral incubator, the "photoinhibitron". The incubator is similar to that previously described (Cullen et al. 1992, Neale et al. 1994), except that quartz cuvettes had a diameter of 2.5 cm and accommodated a sample aliquot of 5-10 ml. Sets of ten cuvettes were used for each spectral treatment, defined by 6.5 x 16.5 cm pieces of glass cutoff filters. The filter types were WG280, WG295, WG305, WG320, WG335, LG350, LG370, and GG400 (WG,GG-Schott,Duryea, PA; LG-Corion, Franklin, Massachusetts). Different intensities were obtained using neutral density screens. Illumination was provided by a 2.5 kW Xe arc lamp and temperature was regulated to -1.0 ± 1 °C with a circulating water bath.

Spectral irradiance was measured using a radiometer system previously described (Cullen & Lesser 1991), except that the spectrograph was operated in scanning mode (200 nm min^{-1}) and the detector was a 1P28B photomultiplier. Estimation of the BWFs based on equations 5-7 was accomplished as previously described (Cullen & Neale 1997, Neale 2000).

A pulse amplitude modulated (PAM) fluorometer (Walz, Effeltrich, Germany) with a high-sensitivity detector (Schreiber 1994) was used to measure the time course in change of the photochemical efficiency of photosystem II as previously described (Neale et al. 1998a). The PAM fluorometer measures the steady-state in vivo chlorophyll fluorescence (F_s) of phytoplankton during illumination with actinic irradiance (PAR only, or UV-PAR). At thirty second intervals a saturating flash (400 ms pulse duration) was applied to obtain a maximum yield (F'_m). The relative efficiency of excitation energy capture by photosystem II (ψ_{PSII}) is calculated as F'_v/F'_m, where $F'_v = (F'_m - F_s)$. Active fluorescence measurements of ψ_{PSII} have been shown to be highly correlated with the overall efficiency (ψ_p), and thus rate, of photosynthesis (Genty et al. 1989). The cuvette holder was modified to accommodate coolant from a circulating water bath so that temperature could be maintained at -1.0 ± 1 °C. For each sample, there was an initial ten minute period without actinic illumination, followed by illumination with PAR only (GG400 filter +copper sulfate solution). PAR was increased to a saturating irradiance (ca. 80 W m^{-2} PAR), until F'_v/F'_m was nearly constant. Once steady state F'_v/F'_m was reached (after 10-20 min exposure), kinetics of UV effects were observed through the decrease in F'_v/F'_m upon supplementing the PAR illumination with UV by replacing the GG400 filter with UV transparent Plexiglas.

RESULTS

Model development

The comparison between the BWF_E and BWF_H models is dependent on the time scale, thus we chose two time-scales that are relevant to processes in the aquatic environment. One is a fast time-scale of a few minutes, over which damage processes will dominate and the other is a long time-scale of one hour, over which both damage and repair processes (when present) will contribute. The choice of time-scales was influenced by the frequent observation that when repair is active, time-courses of photosynthesis under UV exposure approach a steady-state in about 15-20 min (e.g., Lesser et al. 1994). Thus, the two time-scales represent the responses before and after steady-state is attained as schematically illustrated in Fig. 1.

In deriving the comparison over short time-scales, the problem to resolve is how to derive a rate from the BWF_E, since the BWF_H is already a rate of change. The rate of change of photosynthesis in the case where damage and repair are both active is described by equation 3. The general solution to this differential equation (Lesser et al. 1994, Neale 2000) is

$$\frac{P(t)}{P_0} = \frac{r}{(k+r)} + \frac{k}{(k+r)} e^{-(k+r)t} \quad (8)$$

This equation describes both time courses shown in Fig. 1 depending on r. The equation simplifies to the cumulative exposure model (BWF_H) when r is zero by equating H^*_{inh} to product of time and the rate of damage (k t). On the other hand, equation 8 simplifies to the steady-state model (BWF_E) for large time, t ($t > \frac{1}{k+r}$).

This general equation provides a basis for linking together the two models. By comparing equation 4 and equation 5 it is clear that $E^*_{inh} = k/r$.

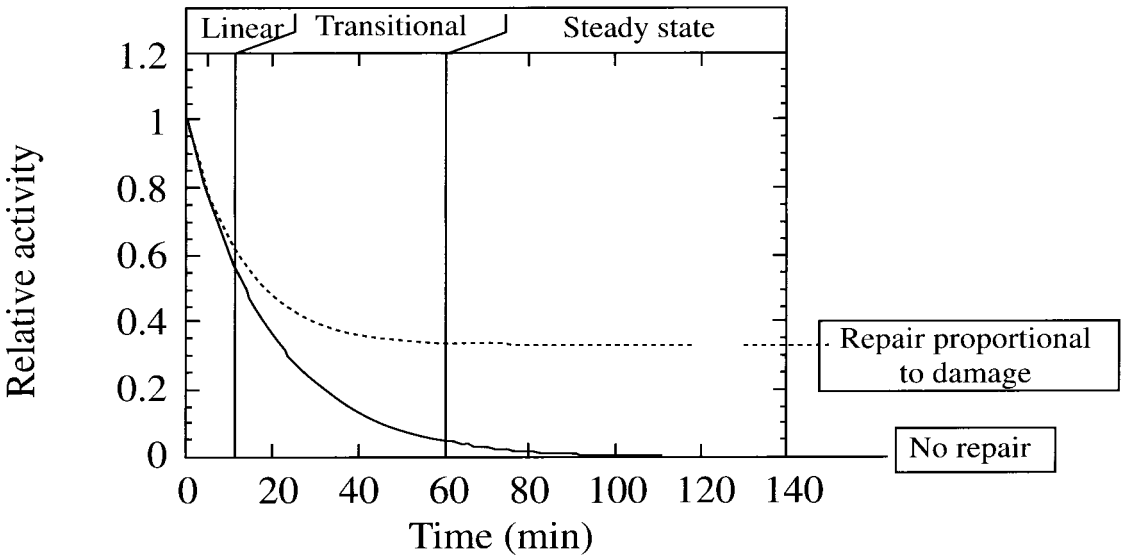

Fig. 1: Hypothetical time courses of UV damage (e.g., inhibition of photosynthesis) to illustrate how the presence of repair affects UV responses. Solid line: Case of no repair, activity decreases to zero (equation 2); small dashes: repair is active and proportional to number of damaged sites (equation 8), activity decreases to a steady state. In these examples the rate of damage (k) is 0.05 min^{-1} and the rate of repair (r) is 0.025 min^{-1}. Labels above the plot indicate time-scale dependence: for short exposures (< 15 min in this case), response is approximately linear; for long exposures (> 30 min) steady-state levels apply, for intermediate time-scales (15-30 min), the transitional (non-linear) kinetics apply.

Curvas hipotéticas de dependencia de inhibición fotosintética respecto al tiempo de daño causado por la radiación UV, demostrando como la presencia de la recuperación afecta la respuesta a UV. Linea sólida: caso de no recuperación, hasta que la actividad disminuye a cero (ecuación 2); rayas: caso de recuperación activa y proporcional al numero de sitios dañados. En estos casos, la velocidad de daño (k) es 0.05 min^{-1} y la velocidad de recuperación (r) es 0.025 min^{-1}. Encima de la gráfica se indica el tipo de dependencia con el tiempo: para exposiciones cortas (< 15 min en este caso) la respuesta es aproximadamente lineal; para exposiciones largas (> 30 min) la actividad está en estado de equilibrio; para exposiciones intermedias (15-30 min) la cinética es transitoria (no lineal).

Thus, given estimates of E^*_{inh} and r, we can solve for k. One way to estimate r when the BWF_E is already known is through measurements of the time course of change in photosynthesis. Since the time for transition to steady-state is on the order of 15 min, fluorescence based approaches are usually needed. By fitting equation 8 to the time course, we defined a rate of transition to steady state ($m\ s^{-1}$) with m = k + r. From this we calculated $r = m/(1 + E^*_{inh})$. Assuming that r is constant under all irradiance regimes, we defined a spectral damage weighting (ε_k) as $\varepsilon_k = \varepsilon_E \times r \times 10^3$. The constant of 10^3 is introduced because ε_E is usually in units of inverse mW m^{-2}, whereas ε_k is defined in units of inverse J m^{-2} so that it can be compared with ε_H.

To make a comparison at the longer time scale (1 h), a transformation is now needed for the BWF_H, as the BWF_E already represents effects at any time scale long enough for an equilibrium to be attained. For this comparison with the BWF_E, we would like to know the inhibitory effect the BWF_H represents under the same irradiance of UV over a 1 h exposure. Application of both the BWF_E and BWF_H to a UV spectrum result in a dimensionless inhibitory exposure (E^*_{inh} and H^*_{inh}), but this weighted exposure is translated to effect through different ERCs, equation 5 for the BWF_E and equation 7 for the BWF_H. Comparison of the two ERCs showed that for the same weighted exposure, the hyperbolic function tends to give a somewhat higher P/P_0 (Fig. 2). In effect, H^*_{inh} has to be about 32 % higher than E^*_{inh} to result in about the same predicted relative decrease in photosynthesis or, equivalently, the effect of a 1 h exposure is 80 % (1/1.32) of a numerically equivalent weighted exposure based on ε_E. This equivalence is approximate, after adjustment the two curves agree within a couple percent of P_0. Overall, the transformation gives a weight for one hour exposure $\varepsilon_{H\text{-}1}$, as $\varepsilon_{H\text{-}1} = 0.80 \times \varepsilon_H \times 3.6$. The constant 3.6 is used to give $\varepsilon_{H\text{-}1}$ in units of inverse mW h^{-1} m^{-2} to agree with the units of ε_E.

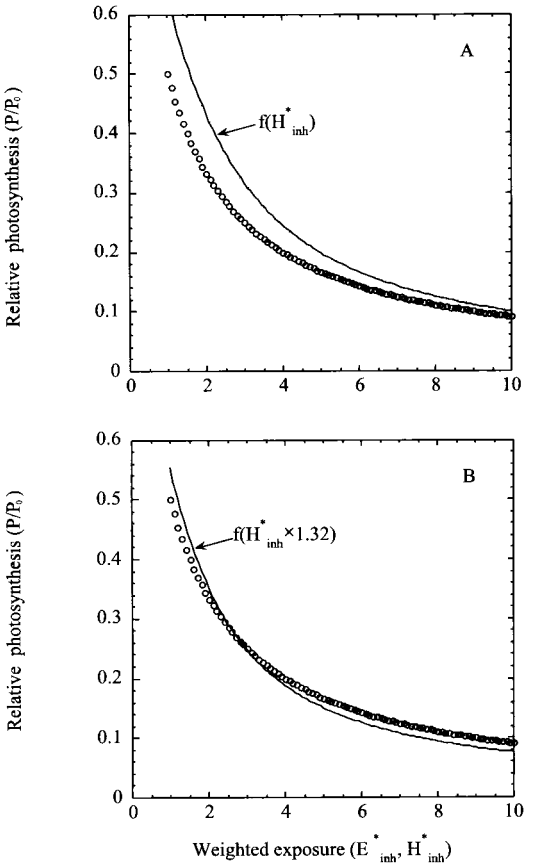

Fig. 2: Relationship between effect and exposure for two types of exposure-response curves (ERCs). Circles: ERC for steady-state photosynthetic rate (P, relative to an initial rate, P_0) as a function of weighted irradiance (E^*_{inh}, dimensionless), i.e., $1/(1+ E^*_{inh})$ (equation 5); solid line: ERC for mean photosynthetic rate (P/P_0) as a function of cumulative exposure (H^*_{inh}, dimensionless), i.e., $f(H^*_{inh}) = (1-\exp(- H^*_{inh}))/ H^*_{inh}$ (equation 7). (A) Effect as a function of unmodified exposure; (B) effect when H^*_{inh} is multiplied by 1.32 before the evaluation of the cumulative exposure ERC (equation 7), i.e., $f(H^*_{inh} x1.32) = (1-\exp(- H^*_{inh} x1.32))/(H^*_{inh} x1.32)$. The scaling factor for H^*_{inh} brings the two ERCs into fairly close agreement.

Relación entre efecto y exposición de dos tipos de curvas de inhibición de fotosíntesis en respuesta a la exposición (ERCs). Círculos: ERC correspondiente a velocidades de fotosíntesis en el estado de equilibrio (P, relativo a la velocidad de fotosíntesis inicial, P_0) en función de la luz efectiva (E^*_{inh}, sin unidades), i.e., $1/(1+ E^*_{inh})$ (ecuación 5); línea sólida: ERC correspondiente a velocidades de fotosíntesis promedio en función de la exposición acumulativa (H^*_{inh}, sin unidades) (ecuación 7). (A) Efecto en función de exposición sin modificaciones; (B) efecto en función de exposición acumulativas multiplicado por 1.32 antes de la evaluación de ERC (ecuación 7), i.e., $f(H^*_{inh} x 1.32) = (1-\exp(- H^*_{inh} x 1.32))/(H^*_{inh} x 1.32)$. Los dos ERCs coinciden bien con el factor de escala para H^*_{inh}.

Application to BWFs for Antarctic Phytoplankton

The time scale of transition to steady state for UV inhibition of photosynthesis was defined by monitoring the time course of change in PSII efficiency (F'_v/F'_m) using a PAM fluorometer during exposure to UV and PAR (Fig. 3). An example is shown for phytoplankton sampled in the vicinity of Palmer Station , the rate constant for transition to steady-state (m) was 2.73×10^{-3} s^{-1}, equivalent to a time constant (1/m) of about 6 min. In other experiments, the time constant varied between 6 and 12 min, overall quite rapid. To calculate the effective E^*_{inh} during UV exposure, the BWF_E determined in the same assemblage was applied to the spectrum of the actinic irradiance. The E^*_{inh} ranged from 0.6 to 1.1 (n = 3). The inferred r (= m/ E^*_{inh}) was 1.2×10^{-3} s^{-1} on average.

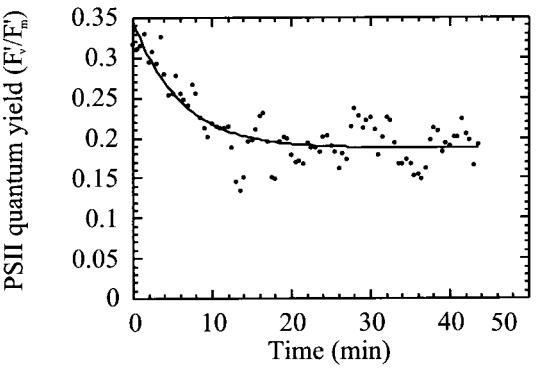

Fig. 3: Time course of F'_v/F'_m (PSII quantum yield) during exposure to PAR and UV irradiance for phytoplankton sampled near Palmer Station, Antarctica, on October 21, 1997. Phytoplankton were first acclimated to PAR (80 W m^{-2}, Xe lamp, $CuSO_4$ solution, GG400 filter), and at time zero the GG400 filter was exchanged with UVT acrylic sheet. PSII quantum yield attains a steady-state after about 10 min exposure indicating a balance between UV damage (inhibition) and repair processes. Filled circles: F'_v/F'_m at 30 s intervals; line: time-course obtained by fitting equation 8 using non-linear regression.

Curso temporal de F'_v/F'_m (rendimiento cuántico del fotosistema II, PSII) durante la exposición a radiación disponible para la fotosíntesis (PAR) y RUV en muestras de fitoplancton tomadas cerca de la Estación Palmer (Antártida) en octubre 21, 1997. Primero, el fitoplancton se aclimató a PAR (80 W m^{-2}, lámpara de Xe, luz filtrada por una solución de $CuSO_4$ y vidrio de Schott GG400), y a la hora "cero" el filtro GG400 se cambió por una lamina acrílica que transmite el paso de RUV. El rendimiento cuántico de PSII llega al estado de equilibrio después de una exposición cercana a 10 min indicando que se ha alcanzado un estado de equilibrio entre los procesos de daño y recuperación. Círculos sólidos: F'_v/F'_m a intervalos de 30 s; línea: curva obtenida de ecuación 8 con parámetros estimados por regresión no lineal.

The BWF_Es for Palmer Station (PAL) assemblages during austral spring 1997 segregated into two groups, a high sensitivity group which corresponded to the period when there was pack ice cover around the station, and a low sensitivity group which was encountered during ice-free periods. A complete discussion of the variation of absolute sensitivity and relative shape of these BWFs will be presented in a separate report. Here we consider the relationship of the average BWF for each group to the average BWF for assemblages in WSC during austral spring 1993 (Neale et al. 1998b).

The factor to convert ε_E to ε_k (= r x 10^3 = 1.2) was applied to the PAL BWFs to calculate ε_k (inverse J m^{-2}) for comparison with average ε_H in the WSC (Fig. 4). This comparison is interpreted as indicative of UV effects over short (minutes) time scale.

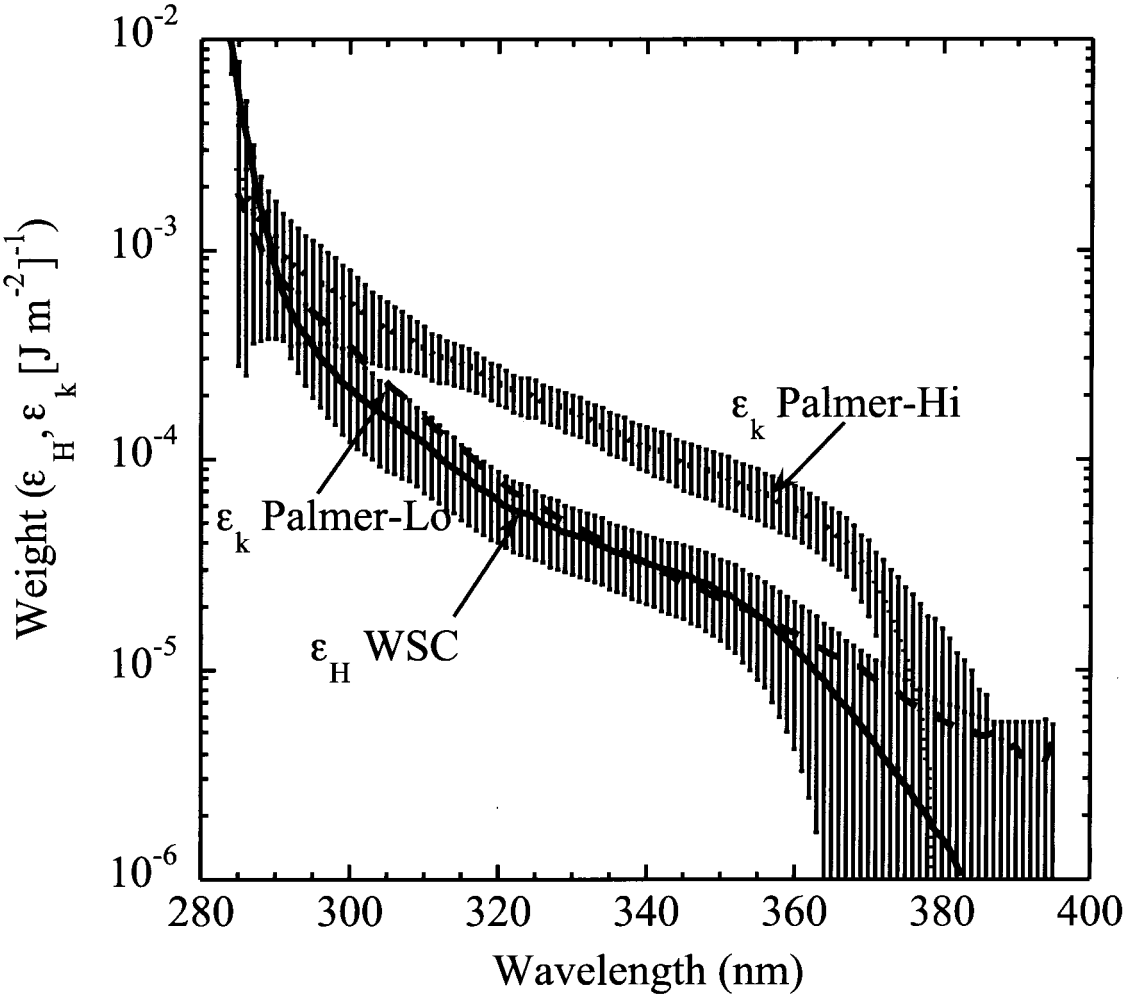

Fig. 4: Biological weighting functions (BWFs) for UV damage (inhibition, inverse J m^{-2}) for Antarctic coastal and pelagic phytoplankton. Solid line: average (± standard deviation) of the BWFs for cumulative exposure (ε_H) determined for the Weddell-Scotia confluence (WSC) assemblages during October-November, 1993 (from Neale et al. 1998b). Long-dashes: average damage weight (ε_k) inferred from BWF_Es for inhibiting irradiance (see Fig. 5) determined for low sensitivity assemblages at Palmer Station October-November, 1997. Short-dashes: average (± standard deviation) damage weight (ε_k) inferred from BWF_Es for inhibiting irradiance (see Fig. 5) determined for high sensitivity assemblages at Palmer Station October-November, 1997.

Funciones espectrales de peso biológico (BWFs) de daño por RUV (inhibición, inverso J m^{-2}) en fitoplancton Antártico costero y pelágico. Línea sólida: promedio (± desviación estándar) de las BWFs de exposición acumulativa (ε_H) determinada en poblaciones de la Confluencia de Weddell-Scotia (WSC) durante octubre-noviembre, 1993 (de Neale et al. 1998b). Rayas largas: promedio de peso de daño (ε_k) inferido de BWF_Es de radiación inhibida (Fig. 5) determinado en las poblaciones de sensibilidad baja de la Estación Palmer, octubre-noviembre, 1997. Rayas cortas: promedio de peso de daño (± desviación estándar) (ε_k) inferido de BWF_Es de radiación inhibida (Fig. 5) determinada en poblaciones de sensibilidad alta de la Estación Palmer, octubre-noviembre, 1997.

BWFs from both PAL and WSC show similar slopes in the UV-A with steeper slopes in the UV-B. In terms of damage rate, the WSC BWFs are most similar to the low sensitivity (open water period) at PAL. The analysis indicated that high sensitivity BWFs from PAL reflected a damage rate about 3.5 times higher than that in the WSC.

In the second comparison, a factor of 2.73 (= 3.6 x 0.80) was applied to the average ε_H from the WSC to obtain a $\varepsilon_{H\text{-}1}$ to compare with ε_E from PAL. This comparison reflects the effect of exposure over a 1-h period. In this case, the average BWF for the high sensitivity (ice cover present) period is similar to the mean $\varepsilon_{H\text{-}1}$ from the WSC. On the other hand, the low sensitivity population had about 30 % of the sensitivity of this other group.

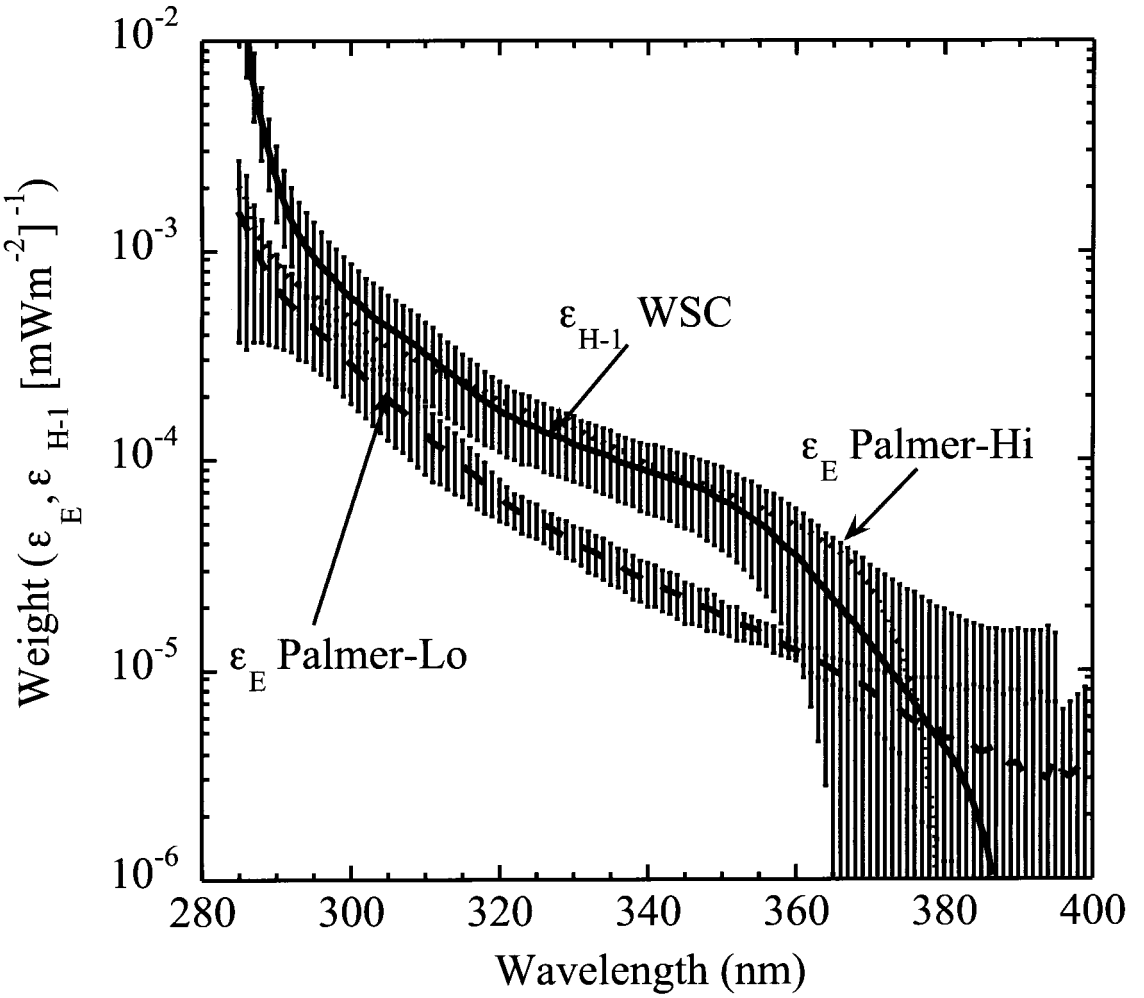

Fig. 5: Biological weighting functions (BWFs) for inhibition by a 1 h exposure to UV (inverse mW m^{-2}) for Antarctic coastal and pelagic phytoplankton. Solid line: average (± standard deviation) of the BWFs for a 1 h exposure ($\varepsilon_{H\text{-}1}$) inferred from average BWF_H (see Fig. 4) of the Weddell-Scotia confluence (WSC) assemblages during October-November, 1993 (from Neale et al. 1998b). Long-dashes: average weight for inhibiting irradiance (ε_E) determined for low sensitivity assemblages at Palmer Station October-November, 1997. Short-dashes: average (± standard deviation) weight (ε_E) for inhibiting irradiance determined for high sensitivity assemblages at Palmer Station.

Funciones espectrales de peso biológico (BWFs) de inhibición por RUV durante 1 h de exposición (inverso mW m^{-2}) en fitoplancton Antárctico costero y pelágico. línea sólida: promedio (± desviación estándar) de las BWFs de exposición de una hora ($\varepsilon_{H\text{-}1}$) inferido de promedio de BWF_Hs (ver Fig. 4) para las poblaciones de la Confluencia de Weddell-Scotia (WSC) durante octubre-noviembre, 1993 (de Neale et al. 1998b). Rayas largas: Promedio de peso de radiación inhibida (ε_E) determinado para poblaciones de sensibilidad baja de la Estación Palmer, octubre-noviembre, 1997. Rayas cortas: promedio de peso (± desviación estándar) de radiación inhibida (ε_E) determinado para poblaciones de sensibilidad baja de la Estación Palmer, octubre-noviembre, 1997.

DISCUSSION

An approach has been developed to partition the relative roles of damage and repair in controlling the sensitivity of marine photosynthesis to UV so that comparisons can be made between assemblages with differing ERCs. The approach is dependent on accurate definition of the time-course of inhibition. It is often difficult to perform this type of experiment, so the requirement is not trivial. The PAM fluorometric approach has the potential to provide good resolution at timescales of around 10 min. However, the sensitivity was too low to produce accurate data in many cases. Sensitivity might be increased by using a Xenon flash as an excitation source (Schreiber et al. 1993). Another problem with the PAM results is the relative decrease in F'_v/F'_m during UV exposure is less than what would be expected based on measurements of photosynthesis as incorporation of ^{14}C-HCO_3. The source of this disagreement (not seen with temperate phytoplankton) needs to be resolved.

The approach was applied in comparing preliminary results for the BWFs of Antarctic phytoplankton in the vicinity of Palmer Station (PAL) to those previously obtained for the Weddell-Scotia Confluence (WSC). Suprisingly, the high sensitivity assemblage found at PAL when there was pack-ice cover had a higher inferred damage rate than that observed in WSC. Over a 1 hour exposure, the two assemblages had about the same sensitivity. It is not known what accounts for the higher sensitivity of the PAL assemblage, however the species composition of phytoplankton was different between the two areas. The WSC was dominated by *Thalassiosira gravida* , a small diatom which forms large colonial aggregates. The PAL assemblage contained a mixture of diatoms species spanning a range of cell sizes. Aggregate forming species such as *T. gravida* were absent from the PAL assemblage.

The low sensitivity assemblage at PAL had a similar rate of damage as the WSC phytoplankton. These two assemblages have in common that they were both exposed to full surface irradiance, though the WSC assemblages inhabited deeply mixed surface layers (Neale et al. 1998b). Again, there were also differences in species composition, with cryptophyte species and a large diatom, *Corethon cryophilum,* important components of the PAL open water assemblage. The presence of active repair in the PAL assemblage lead to a large difference in sensitivity compared to WSC over a 1-h period. The higher rate of repair in the PAL assemblage may be part of physiological acclimation to the generally higher average light intensities that phytoplankton experience under open water conditions in the shallow areas around Palmer Station. Also, the species which dominated during the open water period may have inherently high capacities for counteracting UV damage. *C. cryophilum* had the second lowest sensitivity for UV damage to nuclear DNA in the presence of photoreactive light among nine Antarctic diatoms examined by Karentz et al. (1991).

The rate at which photosynthesis by the WSC assemblage is inhibited during UV exposure was inferred from the ε_H This coefficient was estimated based on a 1-h incubation period, so it is a measure of the average rate of change in photosynthesis during the incubation. In fact, the time course of inhibition may be more complex than a simple survival curve, with faster rates of decline when exposure begins with subsequent slowing due to weak repair. This would affect the difference between WSC and PAL damage weights inferred in the present analysis. Also, the analysis assumes that the specific repair rate is not a function of UV spectral composition and was identical between high and low sensitivity assemblages. These assumptions are being examined further through additional experiments conducted in WSC and at Palmer Station in 1998 and 1999.

Initial efforts to develop BWFs for the inhibition of photosynthesis by Antarctic phytoplankton have produced quite variable results (Neale 2000). The shape of the BWF (Neale et al. 1994) and overall sensitivity to UV inhibition (Neale et al. 1994, Vernet et al. 1994) varies between populations from diverse Antarctic environments. Variation in UV-A sensitivity appears to be greater than variation in UV-B sensitivity (Behrenfeld et al. 1993, Neale et al. 1998b). To better understand the causes of this variation, BWFs need to be systematically related to differences in environmental conditions and species composition. The methods demonstrated in this report will assist such an analyses by enabling broad comparisons between BWFs for phytoplankton in Antarctic and other environments.

LITERATURE CITED

BANASZAK AT & PJ NEALE (2001) UV Sensitivity of photosynthesis in phytoplankton from an estuarine environment. Limnology and Oceanography 46: 000-000.

BEHRENFELD MJ, JW CHAPMAN, JT HARDY & HI LEE (1993) Is there a common response to ultraviolet-B radiation by marine phytoplankton? Marine Ecology Progress Series 102: 59-68.

BÜHLMANN B, P BOSSARD & U UEHLINGER (1987) The influence of longwave ultraviolet radiation (u.v. A) on the photosynthetic activity (^{14}C-assimilation) of phytoplankton. Journal of Plankton Research 9: 935-943.

CALDWELL MM, LB CAMP, CW WARNER & SD FLINT (1986) Action spectra and their key role in assessing biological consequences of solar UV-B radiation change. In: Worrest RC & MM Caldwell (eds) Stratospheric ozone reduction, solar ultraviolet radiation and plant life: 87-111. Springer-Verlag, New York, New York.

COOHILL TP (1989) Ultraviolet action spectra (280 to 380 nm) and solar effectiveness spectra for higher plants. Photochemistry and Photobiology 50: 451-457.

COOHILL TP (1991) Photobiology school: action spectra again? Photochemistry and Photobiology 54: 859-870.

CULLEN JJ & MP LESSER (1991) Inhibition of photosynthesis by ultraviolet radiation as a function of dose and dosage rate: results for a marine diatom. Marine Biology 111: 183-190.

CULLEN JJ & PJ NEALE (1997) Biological weighting functions for describing the effects of ultraviolet radiation on aquatic systems. In: Häder DP (ed) Effects of ozone depletion on aquatic ecosystems: 97-118. R. G. Landes, Austin, Texas.

CULLEN JJ, PJ NEALE & MP LESSER (1992) Biological weighting function for the inhibition of phytoplankton photosynthesis by ultraviolet radiation. Science 258: 646-650.

FURGAL JA & REH SMITH (1997) Ultraviolet radiation and photosynthesis by Georgian Bay phytoplankton of varying nutrient and photoadaptive status. Canadian Journal of Fisheries and Aquatic Sciences 54: 1659-1667.

GENTY B, JM BRIANTAIS & N BAKER (1989) The relationship between the quantum yield of photosynthetic electron transport and quenching of chlorophyll fluorescence. Biochimica et Biophysica Acta 990: 87-92.

HARM W (1980) Biological effects of ultraviolet radiation. Cambridge University Press, Cambridge, United Kingdom. 216 pp.

HELBLING EW, V VILLAFAÑE, M FERRARIO & O HOLM-HANSEN (1992) Impact of natural ultraviolet radiation on rates of photosynthesis and on specific marine phytoplankton species. Marine Ecology Progress Series 80: 89-100.

KARENTZ D, JE CLEAVER & DL MITCHELL (1991) Cell survival characteristics and molecular responses of Antarctic phytoplankton to ultraviolet-B radiation. Journal of Phycology 27: 326-341.

LESSER MP, JJ CULLEN & PJ NEALE (1994) Carbon uptake in a marine diatom during acute exposure to ultraviolet B radiation: relative importance of damage and repair. Journal of Phycology 30: 183-192.

MASKE H (1984) Daylight ultraviolet radiation and the photoinhibition of phytoplankton carbon uptake. Journal of Plankton Research 6: 351-357.

NEALE PJ (2000) Spectral weighting functions for quantifying the effects of ultraviolet radiation in marine ecosystems. In: de Mora SJ, S Demers & M Vernet (eds) The effects of UV radiation on marine ecosystems: 73-100. Cambridge University Press, Cambridge, United Kingdom.

NEALE PJ, AT BANASZAK & CR JARRIEL (1998a) Ultraviolet sunscreens in dinoflagellates: mycosporine-like amino acids protect against inhibition of photosynthesis. Journal of Phycology 34: 928-938.

NEALE PJ, JJ CULLEN & RF DAVIS (1998b) Inhibition of marine photosynthesis by ultraviolet radiation: variable sensitivity of phytoplankton in the Weddell-Scotia Sea during the austral spring. Limnology and Oceanography 43: 433-448.

NEALE PJ, MP LESSER & JJ CULLEN (1994) Effects of ultraviolet radiation on the photosynthesis of phytoplankton in the vicinity of McMurdo Station (78° S). In: Weiler CS & PA Penhale (eds) Ultraviolet radiation in Antarctica: measurement and biological effects: 125-142. American Geophysical Union, Washington, District of Columbia.

PRÉZELIN BB, NB BOUCHER & RC SMITH (1994) Marine primary production under the influence of the Antarctic ozone hole: Icecolors '90. In: Weiler CS & PA Penhale (eds) Ultraviolet radiation in Antarctica: measurement and biological effects: 159-186. American Geophysical Union, Washington, District of Columbia.

SCHREIBER U, C NEUBAUER & U SCHLIWA (1993) PAM fluorometer based on medium frequency pulsed Xe-flash measuring light: a highly sensitive tool in basic and applied photosynthetic research. Photosynthesis Research 10: 51-62.

STEEMANN-NIELSEN E (1964) On a complication in marine productivity work due to the influence of ultraviolet light. Journal du Conseil International pour l'Exploration de la Mer 22: 130-135.

VERNET M, EA BRODY, O HOLM-HANSEN & BG MITCHELL (1994) The response of Antarctic phytoplankton to ultraviolet radiation: absorption, photosynthesis, and taxonomic composition. In: Weiler CS & PA Penhale (eds) Ultraviolet radiation in Antarctica: measurement and biological effects: 143-158. American Geophysical Union, Washington, District of Columbia.

VILLAFAÑE VE, EW HELBLING, O HOLM-HANSEN & BE CHALKER (1995) Acclimatization of Antarctic natural phytopolankton assemblages when exposed to solar ultraviolet radiation. Journal of Plankton Research 17: 2295-2306.

VINCENT WF & PJ NEALE (2000) Mechanisms of UV damage in aquatic organisms. In: de Mora SJ, S Demers & M Vernet (eds) The effects of UV radiation on marine ecosystems: 149-176. Cambridge University Press, Cambridge, United Kingdom.

WEILER CS & PA PENHALE (eds) (1994) Ultraviolet radiation in Antarctica: Measurement and biological effects. American Geophysical Union, Washington, District of Columbia. 257 pp.

Associate Editor: V. Montecino
Received April 12, 2000; accepted January 3, 2001